

Tight-binding theory of surface spin states on bismuth thin films

Kazuo Saito, Hirokatsu Sawahata, Takashi Komine and Tomosuke Aono

Faculty of Engineering, Ibaraki University

*Hitachi 316-8511, Japan**

(Dated: May 1, 2022)

The surface spin states for bismuth thin films were investigated using an sp^3 tight-binding model. The model explains the experimental observations using angle-resolved photoemission spectroscopy, including the Fermi surface, the band structure with Rashba spin splitting, and the quantum confinement in the energy band gap of the surface states. A large out-of-plane spin component also appears. The surface states penetrate inside the film to within approximately a few bilayers near the Brillouin-zone center, whereas they reach the center of the film near the Brillouin-zone boundary.

Introduction.— Spin-orbit interaction (SOI) induces spin splitting in the absence of an external magnetic field on a two-dimensional (2D) system, i.e., Rashba spin splitting [1], which has been an indispensable element of spintronics physics and devices [2]. The Rashba effect is expected on crystal surfaces due to their inversion asymmetry. For example, Rashba spin splitting has been observed on the Au(111) surface [3–5]. Bismuth (Bi) is a group V semimetal with a large SOI due to the heavy mass of the Bi atom; therefore, the surface of Bi crystals is an ideal system to observe a strong Rashba effect [6].

Angle-resolved photoemission spectroscopy (APRES) experiments have been reported for the Bi surface accompanied with first-principles band calculations [7–19]. The surface states have a hexagonal electron pocket around the $\bar{\Gamma}$ point and six-fold hole pockets [7, 9, 10, 16, 19]. The first-principles band calculations showed that these two surface states are spin-split bands [8, 10], and this Rashba splitting has been confirmed experimentally [12–14]. In addition, the surface spin orientation has been elucidated, and in particular, a giant out-of-plane spin polarization was reported [15]. The band structure is dependent on the film thickness because of the quantum confinement effect [10, 12, 17].

Although the first-principles band calculations have already revealed the Fermi surface and the energy band structure [8, 10, 12, 20], no systematic analysis for comparison with the reported experimental results has been conducted to date. Here, we approach this issue using an sp^3 tight-binding model that reproduces the band structure of bulk Bi proposed by Liu and Allen [21]. This model has been applied to discuss the topological and non-topological phases of the surface states of pure Bi and Sb [22], and $\text{Bi}_{1-x}\text{Sb}_x$ [23], as well as two-dimensional Bi [24]. We add extra surface hopping terms [25, 26] that were originally proposed to explain the Au(111) surface states. This model will allow us to confirm whether the ARPES results originate from the surface effect. In addition, it is straightforward to see the effects of quantum confinement because the film thickness can be easily changed and the electronic states both

inside the film and at the surface can be analyzed. We can thus give a systematic survey of the experimental results by taking advantage of these points.

Model Hamiltonian.— Bismuth has a rhombohedral Bravais lattice with two atoms per unit cell, forming a bilayer (BL) structure, as shown in Fig. 1(a). A Bi thin film is obtained by stacking the BLs along the (111) direction, such as the z -axis depicted in Fig. 1(b). The surface is thus parallel to the xy plane. The uppermost and lowermost BLs are in contact with a vacuum.

We first construct a model Hamiltonian for the Bi thin film. For this purpose, the sp^3 tight-binding model proposed for the bulk Bi crystal [21] is adapted to the Bi thin film. There are s -, p_x -, p_y -, and p_z -orbitals with spin index σ on each atom. The hopping terms among the atomic orbitals are decomposed into inter- and intra-BL hopping terms. The inter-BL hopping term H_{21-2} , consists of the nearest-neighbor hopping term in the bulk Bi Hamiltonian, whereas the intra-BL hopping term consists of two parts, H_{11} and H_{12-1} , with the third and second nearest-neighbor hopping terms in the bulk model, respectively. The Fermi energy is set to zero.

There is a surface potential gradient on the surface BL along the z axis between the surface Bi atoms and the vacuum. The surface Rashba effect is induced by the contribution of this potential gradient [25, 26]. In terms of the sp^3 tight-binding model, this is described by the following spin independent hopping terms between the nearest-neighbors sites, \mathbf{R}_i and \mathbf{R}_j [25, 26]:

$$t_{\alpha\beta} = \begin{cases} \gamma_{pp} \cos \theta_{ij} & , (\alpha, \beta) = (p_x, p_z) \text{ or } (p_z, p_x), \\ \gamma_{pp} \sin \theta_{ij} & , (\alpha, \beta) = (p_y, p_z) \text{ or } (p_z, p_y), \\ \gamma_{sp} & , (\alpha, \beta) = (s, p_z) \text{ or } (p_z, s), \end{cases} \quad (1)$$

where θ_{ij} is the azimuthal angle between $\mathbf{R}_i - \mathbf{R}_j$ and the x -axis, and γ_{pp} and γ_{sp} are the hopping matrix elements of the Hamiltonian. Note that those hopping terms are zero in the bulk Bi crystal model because of the inversion symmetry. We assume that the surface hopping terms (1) appear only on the uppermost atomic layer, the first atomic layer of the uppermost BL, and the lowermost atomic layer with $-\gamma_{sp/pp}$, because the surface field points in the opposite direction at the lowermost layer. The values of γ_{sp} and γ_{pp} remain to be determined at this stage.

* aono@mx.ibaraki.ac.jp

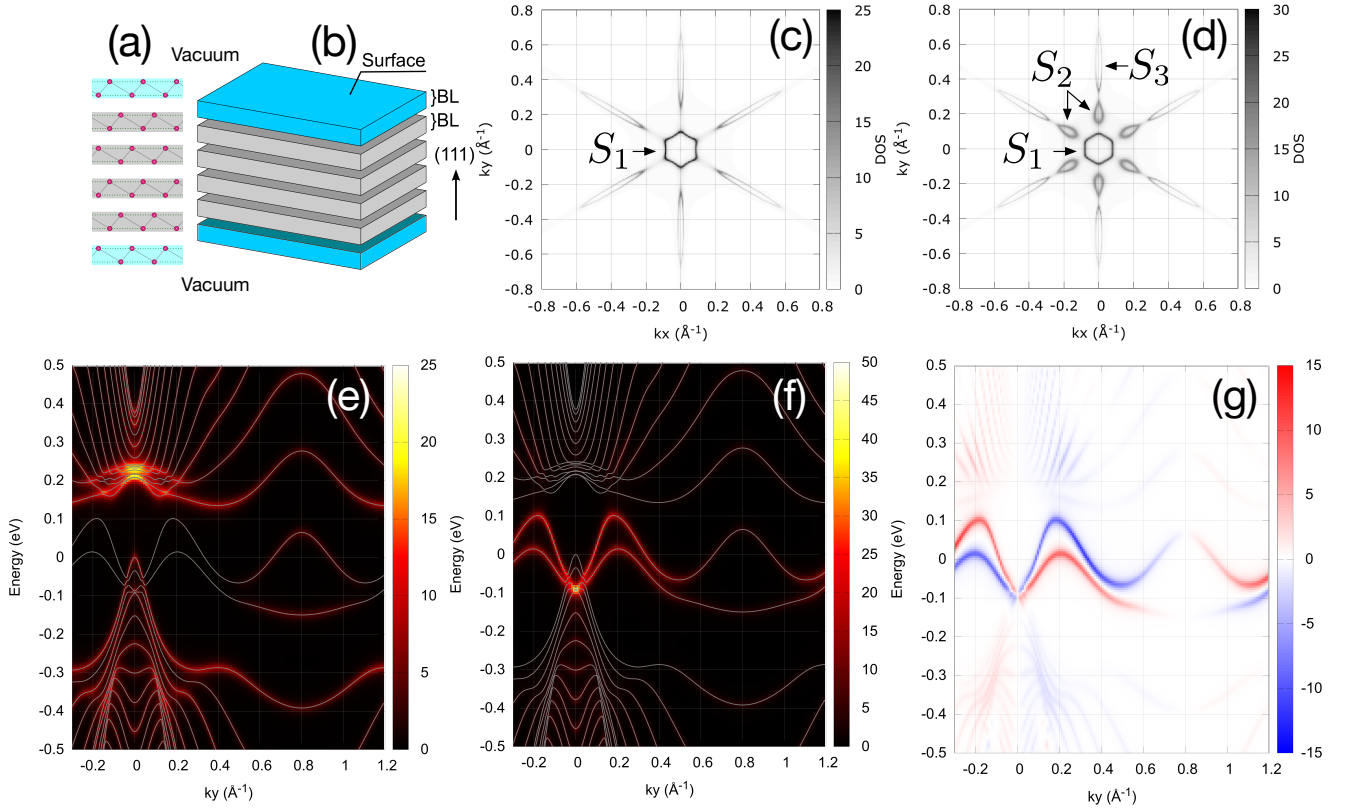


FIG. 1. (Color online) (a) Bismuth crystal structure. (b) Schematic view of Bi thin film. (c, d) Surface BL density of states at the Fermi energy $\rho(1, 0, k_x, k_y)$ of a 16 BL film with (c) $\gamma_{pp/sp} = 0$, and (d) with $\gamma_{sp} = 0.45$ and $\gamma_{pp} = -0.27$. (e, f) Energy band structure along the Γ -M line for the (e) middle BL and (f) the surface BL. The white lines represent the eigenvalues of H . (g) Spin resolved band structure for (f).

The total Hamiltonian of the thin film H is therefore represented by the following matrix form:

$$H = \begin{pmatrix} H_{s11} & H_{12-1} & & & & \\ H_{21-1} & H_{11} & H_{21-2} & & & \\ & H_{12-2} & H_{11} & H_{12-1} & & \\ & & H_{21-1} & H_{11} & & \\ & & & & \ddots & \ddots \\ & & & & & H_{11} & H_{12-1} \\ & & & & & H_{21-1} & H'_{s11} \end{pmatrix}, \quad (2)$$

where H_{s11} is the Hamiltonian for the uppermost atomic layer, which includes the surface hopping terms (1) in addition to H_{11} , while H'_{s11} is the Hamiltonian that includes the surface hopping terms (1) with $-\gamma_{pp/sp}$. The size of the matrix is thus $16n \times 16n$ when the number of the BLs is n . The Hamiltonian (2) is a function of the wave vectors k_x and k_y : $H = H(k_x, k_y)$.

Calculation of density of states.— The density of states and the band structure of the thin film is obtained from the retarded Green function matrix $G(E, k_x, k_y)$ with energy E defined by

$$G(E, k_x, k_y) = [E + i\delta - H(k_x, k_y)]^{-1} \quad (3)$$

with $\delta = 1.0 \times 10^{-2}$ in the numerical calculations. The

density of states in the i th BL is defined by

$$\rho(i, E, k_x, k_y) = -\frac{1}{\pi} \text{Tr} \text{Im} G(E, k_x, k_y), \quad (4)$$

where Tr stands for the trace over the orbitals and the spin only on the i th BL ($i = 1$ for the uppermost BL). In a similar way, the spin resolved density of states $s_\alpha(i, E, k_x, k_y)$ ($\alpha = x, y, z$) is given by

$$s_\alpha(i, E, k_x, k_y) = -\frac{1}{\pi} \text{Tr} s_\alpha \text{Im} G(E, k_x, k_y), \quad (5)$$

where s_α is the Pauli spin matrix that acts on the four orbital states. The eigenvalues of H are also calculated to show the entire band structure of the film.

Parameter fitting.— In the following, γ_{sp} and γ_{pp} are treated as fitting parameters. To fix these values, we take a phenomenological approach: We first calculate the density of states on the surface BL and the band structure for various values of $\gamma_{sp/pp}$ and then compare them with the ARPES experimental results [7, 8, 10, 11, 16, 19] to find the best selection. This scheme was successful and led to $\gamma_{sp} = 0.45$, and $\gamma_{pp} = -0.27$. The numerical results appear similar near these values. Note that these values are the same order of magnitude as the hopping

matrix elements between the second and third nearest neighbors given in Ref. [21].

The presence of the surface terms (1) is essential to explain the observed Fermi surface. Figures 1(c) and (d), show the density of states on the surface BL at the Fermi energy $\rho(1, 0, k_x, k_y)$ for the 16 BL thin film without and with the surface hopping terms, respectively. In both cases, a hexagonal electron pocket appears around the $\bar{\Gamma}$ point designated by S_1 . Qualitative differences arise outside of S_1 ; with the surface hopping term, there are six hole lobes and six extra electron lobes, designated by S_2 , and S_3 , respectively, while S_2 is missing without the surface hopping term. The ARPES experiments show the presence of S_2 , which confirms that the surface terms (1) play a central role in the formation of the Fermi surface.

Band structure.— Next, we discuss the energy band structure. Figures 1(e) and (f) show $\rho(i, E, 0, k_y)$ for the middle ($i = 8$) and surface ($i = 1$) BLs, respectively, along the $\bar{\Gamma}$ - \bar{M} line. The eigenvalues of H are also shown as white lines for comparison. On the middle BL, the plot covers most of the eigenvalues, while on the surface BL, the plot appears only in a small fraction of the eigenvalue curves and mostly on two curves near the Fermi energy. The upper curve forms the S_1 and S_3 structures, whereas the lower curve forms the S_2 structure.

The spin resolved band structure illustrates the distinctive features of the surface states, as shown in Fig 1(g). The spin splitting appears near the $\bar{\Gamma}$ point, which is similar to Rashba spin splitting, and it diminishes near \bar{M} . This is consistent with the experimental results and the first-principles band calculations [12, 14]. Thus, the surface states on the Bi film are well described by the phenomenological tight-binding model.

Surface spin states.— Next, we discuss the surface spin texture at the Fermi energy; $s_\alpha \equiv s_\alpha(1, 0, k_x, k_y)$. Figure 2(a) shows the in-plane spin $\mathbf{s}_\parallel = (s_x, s_y)$ distribution. On S_1 , \mathbf{s}_\parallel lies along the pocket structure, while on S_2 , \mathbf{s}_\parallel is almost perpendicular to \mathbf{k} , and the direction of \mathbf{s} is opposite to that on S_1 . The in-plane spin rotations on S_1 and S_2 are similar to those by the Rashba SOI. In addition, $|\mathbf{s}_\parallel|$ along the lobe on S_2 is almost constant. These observations are consistent with previous experimental results [9, 13, 15, 18]. However, the asymmetry of $|\mathbf{s}_\parallel|$ along k_y axis on S_2 [15] is not observed in the present model. Instead of this asymmetry, $|\mathbf{s}_\parallel|$ on S_1 oscillates every 60° , which indicates that the spin structure is not described by a simple Rashba SOI model.

The deviation from the simple Rashba model is clarified by the out-of-plane spin s_z , as shown in Fig. 2(b). There is a relatively large s_z over the S_1 - S_3 structures, where the maximum of $|s_z|$ is approximately 25% of the maximum of $|\mathbf{s}_\parallel|$. Furthermore, s_z changes its sign every 60° . These results are consistent with recent experimental results [15], although larger values of $|s_z|$ are observed in the experiment. In addition, the fine structure of s_z is clarified, where the sign of s_z also changes from S_1 to S_3 in the same manner as \mathbf{s}_\parallel .

We further discuss the presence of the giant s_z com-

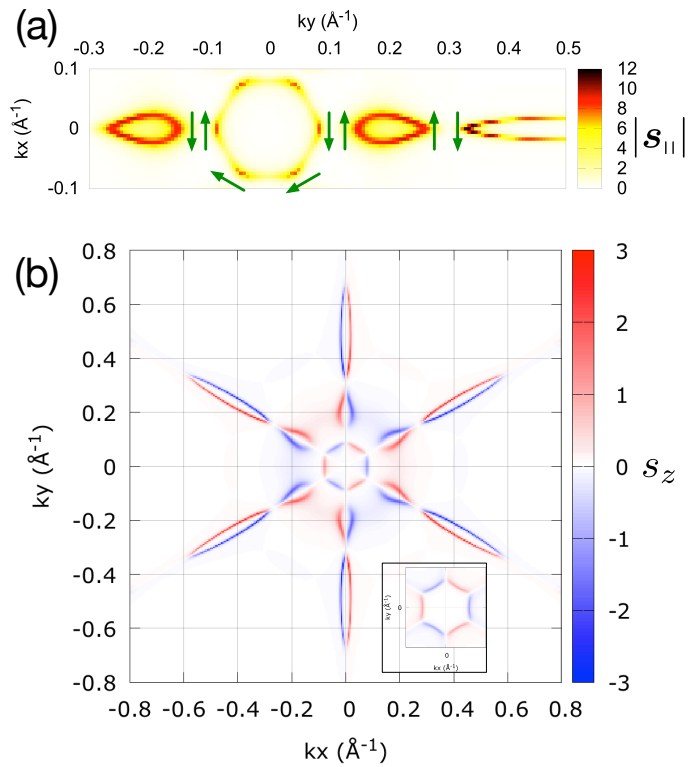


FIG. 2. (Color online) (a) In-plane surface spin magnitude $|\mathbf{s}_\parallel|$. The green arrows indicate the direction of \mathbf{s}_\parallel for representative points. (b) Out-of-plane surface spin s_z . Inset: s_z around the $\bar{\Gamma}$ point without the surface hopping terms and with the same scale as the main figure.

ponent. The first-principles calculations show similar results for s_z with the topological phase of the $\text{Bi}_{1-x}\text{Sb}_x$ crystal [27], where s_z is very small and around 1% of $|\mathbf{s}_\parallel|$, which indicates the spin lies on the two-dimensional surface. Pure Bi ($x = 0$) is in the trivial phase [22, 23, 27]; therefore, large values of s_z may be direct evidence for clarification of the difference between the trivial and topological phases, besides the number of Fermi surface crossings from the zone center to the boundary. To support this point within the proposed model, s_z without the surface hopping term near the $\bar{\Gamma}$ point is shown in the inset of Fig. 2(b). Similar results are obtained both with and without the surface hopping terms. This indicates that the origin of s_z is not from the surface effect, but from the bulk hopping terms and the atomic SOI of Bi itself, which determines the bulk band structure. Thus, the origin of s_z for pure Bi is associated with the bulk band structure, which leads to a trivial phase.

BL number dependence.— Figure 3(a) shows $\rho(1, 0, k_x, k_y)$ for a 40 BL film. Compared with that for the 16 BL film, both S_1 and S_2 structures are unchanged, while the S_3 structure is prolonged towards the \bar{M} point, which is consistent with the experimental results [10, 11]. To examine this difference in detail, we discuss the BL number dependence along the two lines

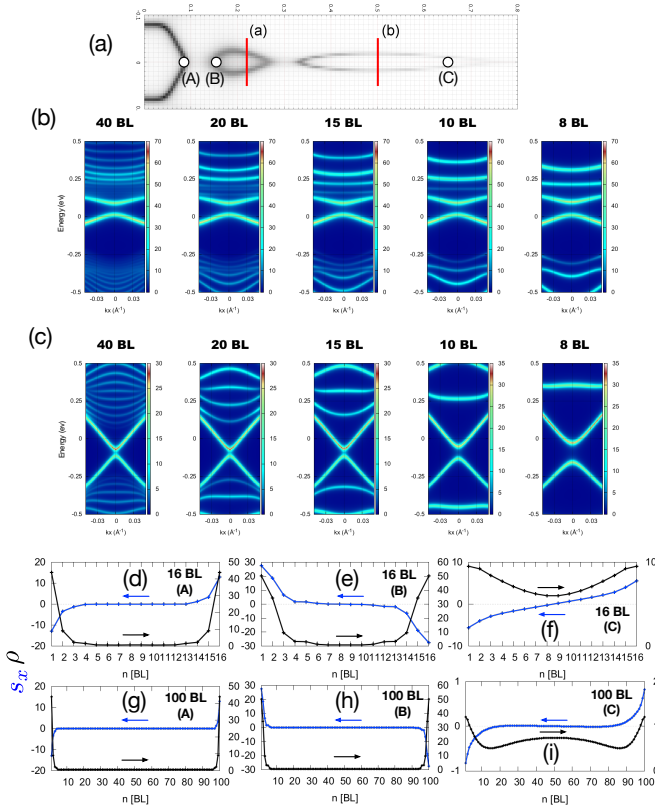


FIG. 3. (Color online) (a) Surface density of states for 40 BL along the $\bar{\Gamma}$ - \bar{M} line with two lines and three points. (b, c) Energy bands for various BL numbers along the lines (a) ($k_y = 0.22$) and (b) ($k_y = 0.5$), respectively. (d-i) The layer-resolved electron densities, $\rho(n)$ and $s_x(n)$, at $k_y = 0.08, 0.16$, and 0.65 , the points (A), (B), and (C) in (a), respectively, for (d-f) 16 BL, and (g-i) 100 BL.

and three points shown in Fig. 3(a).

Figure 3(b) shows $\rho(1, E, 0, k_y)$ in S_2 for various BL numbers along the line (a) shown in Fig. 3(a). The two surface states near the Fermi energy separated by a band gap are not affected by changing the BL number. However, the energy levels away from the Fermi level are under the strong influence of the BL number, which indicates the quantum confinement in the thin film. Fig-

ure 3(c) shows the band structures in S_3 along the line (b) shown in Fig. 3(a). Although the band structure near the Fermi level shows a linear dispersion similar to that for line (a), the band gap clearly decreases as the BL number increases. A similar observation is obtained experimentally [17]. Hence, the surface states are under the strong influence of quantum confinement on S_3 , while they are not on S_2 .

Finally we discuss the surface state penetration inside the thin film. For this purpose, the layer-resolved electron densities, $\rho(n) \equiv \rho(n, 0, 0, k_y)$ and $s_x(n) \equiv s_x(n, 0, 0, k_y)$, are shown in Figs. 3(d-f) and (g-i) for the 16 BL and 100 BL films, respectively, at the three points indicated in Fig. 3(a). All the figures show that the spin on the uppermost and lowermost BLs are in opposite directions, as expected; The spin changes its sign at the middle of the film. The surface states on S_1 penetrate only a few BLs, and a similar result is obtained for the surface states on S_2 with a slightly longer penetration length. The penetration length is unchanged by the film thickness, which confirms they are genuine surface states. On other hand, at S_3 , $\rho(n)$ and $s_x(n)$ decay over 20 BLs, and $\rho(n)$ is finite even at the middle of the film. Thus, the states are no longer simple “surface” states and are under the influence of the quantum confinement inside the film.

Conclusions.— We have shown that an sp^3 tight-binding model with surface hopping terms can explain most of the experimental ARPES observation for bismuth thin films, including the Fermi surface, the spin-resolved band structure with Rashba spin splitting, and the quantum confinement effect in the energy band structure. The model also explains the large out-of-plane spin observed, which originates from the intrinsic Bi crystal structure rather than the surface effect. We have also clearly shown that the surface states penetrate inside the film to within approximately a few BLs near the Brillouin-zone center, whereas they reach the center of the film near the Brillouin-zone boundary.

The authors acknowledge A. Takayama for fruitful discussions and comments on the ARPES experimental results. We also thank J. Ieda for stimulating discussion. This work is partially supported by KAKENHI and the Japan Science and Technology Agency (JST).

[1] Y. A. Bychkov and É. I. Rashba, JETP Lett. **39**, 78 (1984).
[2] R. Winkler, *Spin-orbit coupling effects in two-dimensional electron and hole systems*, 191 (Springer Science & Business Media, 2003).
[3] S. LaShell, B. A. McDougall, and E. Jensen, Phys. Rev. Lett. **77**, 3419 (1996).
[4] G. Nicolay, F. Reinert, S. Hüfner, and P. Blaha, Phys. Rev. B **65**, 033407 (2001).
[5] J. Henk, M. Hoesch, J. Osterwalder, A. Ernst, and P. Bruno, J. Phys. Condens. Matter **16**, 7581 (2004).

[6] P. Hofmann, Progress in Surface Science **81**, 191 (2006).
[7] C. R. Ast and H. Höchst, Phys. Rev. Lett. **87**, 177602 (2001).
[8] Y. M. Koroteev, G. Bihlmayer, J. E. Gayone, E. V. Chulkov, S. Blügel, P. M. Echenique, and P. Hofmann, Phys. Rev. Lett. **93**, 046403 (2004).
[9] T. K. Kim, J. Wells, C. Kirkegaard, Z. Li, S. V. Hoffmann, J. E. Gayone, I. Fernandez-Torrente, P. Häberle, J. I. Pascual, K. T. Moore, A. J. Schwartz, H. He, J. C. H. Spence, K. H. Downing, S. Lazar, F. D. Tichelaar, S. V. Borisenko, M. Knupfer, and P. Hofmann, Phys. Rev. B

- 72**, 085440 (2005).
- [10] T. Hirahara, T. Nagao, I. Matsuda, G. Bihlmayer, E. V. Chulkov, Y. M. Koroteev, P. M. Echenique, M. Saito, and S. Hasegawa, Phys. Rev. Lett. **97**, 146803 (2006).
 - [11] T. Hirahara, T. Nagao, I. Matsuda, G. Bihlmayer, E. V. Chulkov, Y. M. Koroteev, and S. Hasegawa, Phys. Rev. B **75**, 035422 (2007).
 - [12] T. Hirahara, K. Miyamoto, I. Matsuda, T. Kadono, A. Kimura, T. Nagao, G. Bihlmayer, E. V. Chulkov, S. Qiao, K. Shimada, H. Namatame, M. Taniguchi, and S. Hasegawa, Phys. Rev. B **76**, 153305 (2007).
 - [13] T. Hirahara, K. Miyamoto, A. Kimura, Y. Niinuma, G. Bihlmayer, E. V. Chulkov, T. Nagao, I. Matsuda, S. Qiao, K. Shimada, H. Namatame, M. Taniguchi, and S. Hasegawa, New Journal of Physics **10**, 083038 (2008).
 - [14] A. Kimura, E. E. Krasovskii, R. Nishimura, K. Miyamoto, T. Kadono, K. Kanomaru, E. V. Chulkov, G. Bihlmayer, K. Shimada, H. Namatame, and M. Taniguchi, Phys. Rev. Lett. **105**, 076804 (2010).
 - [15] A. Takayama, T. Sato, S. Souma, and T. Takahashi, Phys. Rev. Lett. **106**, 166401 (2011).
 - [16] Y. Ohtsubo, J. Mauchain, J. Faure, E. Papalazarou, M. Marsi, P. Le Fèvre, F. Bertran, A. Taleb-Ibrahimi, and L. Perfetti, Phys. Rev. Lett. **109**, 226404 (2012).
 - [17] A. Takayama, T. Sato, S. Souma, T. Oguchi, and T. Takahashi, Nano Letters **12**, 1776 (2012).
 - [18] A. Takayama, T. Sato, S. Souma, and T. Takahashi, New J. Phys. **16**, 055004 (2014).
 - [19] A. Takayama, T. Sato, S. Souma, T. Oguchi, and T. Takahashi, Phys. Rev. Lett. **114**, 066402 (2015).
 - [20] Y. M. Koroteev, G. Bihlmayer, E. V. Chulkov, and S. Blügel, Phys. Rev. B **77**, 045428 (2008).
 - [21] Y. Liu and R. E. Allen, Phys. Rev. B **52**, 1566 (1995).
 - [22] T. Fukui and Y. Hatsugai, J. Phys. Soc. Jpn. **76**, 053702 (2007).
 - [23] J. C. Y. Teo, L. Fu, and C. L. Kane, Phys. Rev. B **78**, 045426 (2008).
 - [24] S. Murakami, Phys. Rev. Lett. **97**, 236805 (2006).
 - [25] L. Petersen and P. Hedegård, Surface Science **459**, 49 (2000).
 - [26] C. R. Ast and I. Gierz, Phys. Rev. B **86**, 085105 (2012).
 - [27] H.-J. Zhang, C.-X. Liu, X.-L. Qi, X.-Y. Deng, X. Dai, S.-C. Zhang, and Z. Fang, Phys. Rev. B **80**, 085307 (2009).